Uncertainty analysis for the steady-state flows in a dual throat nozzle

Qian-Yong Chen, David Gottlieb, Jan S. Hesthaven [*]

Division of Applied Mathematics, Brown University, Box F, Providence, RI 02912, USA

Abstract

It is well known that the steady state of an isentropic flow in a dual-throat nozzle with equal throat areas is not unique. In particular there is a possibility that the flow contains a shock wave, whose location is determined solely by the initial condition. In this paper, we consider cases with uncertainty in this initial condition and use generalized polynomial chaos methods to study the steady-state solutions for stochastic initial conditions. Special interest is given to the statistics of the shock location. The polynomial chaos (PC) expansion modes are shown to be smooth functions of the spatial variable x, although each solution realization is discontinuous in the spatial variable x. When the variance of the initial condition is small, the probability density function of the shock location is computed with high accuracy. Otherwise, many terms are needed in the PC expansion to produce reasonable results due to the slow convergence of the PC expansion, caused by non-smoothness in random space.
© 2004 Elsevier Inc. All rights reserved.

1. Introduction

In [11] a model for isentropic flow in a dual-throat nozzle with equal throat areas was considered. The steady-state flow was shown to be either completely supersonic, completely subsonic, or a flow containing a shock wave connecting the supersonic branch of the solution to the subsonic branch. The location of the shock wave depends uniquely on the initial condition (see also [3]). The question arises: what can be said about the shock location if there are uncertainties in the initial conditions. While randomness enters through the initial conditions in this problem, random effects can generally enter into practical problems

---

[*] Corresponding author. Tel.: +1 401 863 2671; fax: +1 401 853 1355.
E-mail addresses: cqy@cfm.brown.edu (Q.-Y. Chen), dig@cfm.brown.edu (D. Gottlieb), jan_hesthaven@brown.edu (J.S. Hesthaven).

through boundary conditions, initial conditions, the domain geometry, missing variables, and fluid properties etc. [10,7,18]. Such random effects in the inputs produce stochastic solutions as outputs, requiring new methodologies to model and analyze the impact of such uncertainties.

In our case we are interested in the statistics of derived quantities (e.g., the shock position of a solution). Such are often hard to accurately compute from the first few moments of the solutions. We demonstrate this point with the following diagram (1). Here ξ is a vector of random variables. $\mu(x)$ and $\sigma(x)$ denote the mean and standard variation of $u(x, \xi)$, respectively. $X_s(\xi)$ is the shock location of $u(x, \xi)$. μ_{X_s} and σ_{X_s} are the first two moments of X_s.

$$
\begin{array}{ccc}
u(x, \boldsymbol{\xi}) & \xrightarrow{\text{Statistics}} & \{\mu(x), \sigma(x), \cdots\} \\
\text{Locating Shock} \downarrow & & \downarrow ?? \\
X_s(\boldsymbol{\xi}) & \xrightarrow{\text{Statistics}} & \mu_{X_s}, \sigma_{X_s}, \cdots
\end{array}
\tag{1}
$$

In most practical situations, the deterministic and probabilistic parts of $u(x, \xi)$ cannot be separated (i.e., $u(x, \xi)$ cannot be written into the form $u(x, \xi) = f(x)g(\xi)$). So the shock locating procedure and statistics computation procedure do not commute with each other because of the complexity and nonlinearity of the former. Hence, there is generally no easy way to accurately compute μ_{X_s} and σ_{X_s} from the first few components of $\{\mu(x), \sigma(x), \ldots\}$.

When additional information is being required about the solution, series expansion methods [12,14,7,21,22] appear as a possible choice for the discretization of random fields. However, the correlation function of the solution is often unknown a priori, therefore polynomial chaos methods seem to be suitable in this scenery.

In this paper, we study the model equation of the isentropic flow in a dual-throat nozzle with equal throat areas as introduced in [11]. Generalized polynomial chaos methods are implemented to compute the probability density function (PDF) of the shock location for the cases where the initial conditions are assumed to be different random processes (fields). When exact solutions are not available, we use the basic Monte Carlo (MC) method to validate the results.

The rest of the paper is organized as follows. In Section 2, we recall the basic MC method and generalized polynomial chaos methods. We also discuss boundary conditions issues for the system obtained when introducing the polynomial chaos expansion. Section 3 includes results from the MC method, Hermite and Jacobi polynomial chaos methods for the model equation. The polynomial chaos expansion is shown to converge slowly for functions which are discontinuous in the random space. Finally, we summarize the results of the paper in Section 4.

2. Monte Carlo method and generalized polynomial chaos methods

In this section, we offer a short review of the basic MC method [18] and generalized polynomial chaos methods [5,19,21,22]. We also discuss the issues of boundary conditions for the systems of hyperbolic equations arising from the polynomial chaos approach.

2.1. Monte Carlo method

In the basic MC method, one generates a number of samples of the input stochastic processes, solves the deterministic equations for each sampled input, and computes the statistics of the desired variables from the solutions. One advantage of MC methods is the simplicity, i.e., we only need to execute the code for the deterministic problems with the sampled inputs. It can provide accurate solutions as long as the number

of samples is high enough. A major drawback is the large amount of computing time required when the standard variation of the output is not small, a particular problem when we are more interested in higher moments. Importance sampling and correlation methods can be used to substantially improve the efficiency for certain problems. One can consult the literature [12,18] and references therein for more information on advanced applications of MC methods.

2.2. Generalized polynomial chaos methods

Generalized polynomial chaos methods [19,5,21,22] involve a spectral representation of the stochastic processes (random functions). In particular, stochastic processes are expanded into multi-dimensional orthogonal generalized hypergeometric polynomials [1] of independent identically distributed (iid) random variables ξ. For a specific random process, the corresponding hypergeometric polynomials should be used to achieve optimal accuracy with a minimum number of expansion terms, e.g., Hermite polynomials should be used for Gaussian processes, and Jacobi polynomials should be used for Beta processes (see [19,22] for a complete list).

Generalized hypergeometric polynomials form a complete orthogonal basis of the L_2 space of random variables. The weighted inner product is defined as

$$\langle f(x,\xi),g(x,\xi)\rangle = \int f(x,\xi)g(x,\xi)\omega(\xi)d\xi = E[f(x,\xi)g(x,\xi)],$$

where the weight function $\omega(\xi)$ is the joint PDF of the random variables. In particular, for the n-dimensional Gaussian random variables, ξ,

$$\omega(\xi) = \frac{1}{(2\pi)^n}e^{-(1/2)\xi^T\xi}.$$

As an example, a Gaussian process $u(x,\theta)$ (with x being the spatial or time coordinate) is expressed as

$$u(x,\theta) = \sum_{l=0}^{\infty} u_l(x)\psi_l(\xi(\theta)),$$

where $\xi(\theta)$ is a vector of iid Gaussian random variables with zero mean and unit variance, and the basis functions $\psi_l(\xi(\theta))$ are the normalized (multidimensional) Hermite polynomials given by

$$H_{(n,p)}(\xi_{i_1},\ldots,\xi_{i_p}) = e^{(1/2)\xi^T\xi}(-1)^p\frac{\partial^p}{\partial\xi_{i_1}\cdots\partial\xi_{i_p}}e^{-(1/2)\xi^T\xi} \quad \forall 1 \leq i_1,\ldots,i_p \leq n.$$

In the computations we use the pth order approximation

$$u_P(x,\theta) = \sum_{l=0}^{P} u_l(x)\psi_l^{(n)}(\xi(\theta)), \tag{2}$$

where $P = (n+p)!/n!p!$ and $\xi(\theta) = (\xi_1(\theta),\ldots,\xi_n(\theta))^T$.

The superscript of $\psi_l^{(n)}$ will be omitted if there is no confusion. Note that there is only one zeroth degree polynomial chaos basis function $\psi_0(\xi) = 1$.

Since $\{\psi_i(\xi)\}$ form an orthonormal basis, the polynomial chaos expansion coefficients of $u(x,\xi)$ are given by

$$u_l(x) = \langle u(x,\xi),\psi_l(\xi)\rangle = E[u(x,\xi)\psi_l(\xi)].$$

It is easy to verify that the mean of $u(x,\xi)$ is the zero mode $u_0(x)$, and the variance is $\text{VAR}(u(x,\xi)) = \sum_{i=1}^{+\infty}(u_i(x))^2$. Moreover, one can generate any number of realizations of $u(x,\xi)$ by sampling

in ξ. This makes it possible to compute the statistics of any derived quantity of the solutions once $\{u_i\}$ are known.

2.2.1. Implementation and boundary conditions for hyperbolic equations

A sensitive issue in the application of polynomial chaos methods to hyperbolic equations is the implementation of boundary conditions. The polynomial chaos method leads to a system of equations for the expansion coefficients. This system should remain well posed and in particular should not require boundary conditions at the outflow of the original problem.

Consider the scalar linear hyperbolic equation

$$u_t + a(x,t,\xi)u_x = 0, \quad 0 \leq x \leq \pi, \ t > 0, \tag{3}$$

where $a(x,t,\xi)$ depends on a random vector ξ.

We represent the solution as in (2) and take the approximate coefficient as $a_P(x,t,\xi) = \sum_{l=0}^{P} a_l(x,t)\psi_l(\xi)$. A standard Galerkin procedure yields a system

$$\frac{\partial u_k}{\partial t} + \sum_{i,j=0}^{P} a_i e_{ijk} \frac{\partial u_j}{\partial x} = 0, \quad k = 0,\ldots,P,$$

where

$$e_{ijk} = E[\psi_i \psi_j \psi_k]:$$

In matrix form we have

$$\mathcal{U}_t + A\mathcal{U}_x = 0, \tag{4}$$

where $\mathcal{U} = (u_0(x,t),\ldots,u_P(x,t))^{\mathrm{T}}$ and the matrix $A = (A_{i,j})$ has elements

$$A_{i,j} = \sum_{l=0}^{P} a_l e_{ijl}, \quad 0 \leq i,j \leq P:$$

Thus, the scalar equation (3) for the random function $u(x,t,\xi)$ is transformed to the system (4) of several deterministic unknowns: $\{u_0(x,t),\ldots,u_P(x,t)\}$. We can determine the nature of the system:

Theorem 1. The system (4) is symmetric hyperbolic. Moreover, if $a_P(x,t,\xi) \geq (\leq) \, 0$ for all ξ at a point (x,t), then the matrix A is positive (negative) semi-definite at this point.

Proof. The symmetry of the matrix A follows directly from the definition of (e_{ijl}). Given any real vector $b = (b_0,\ldots,b_P)$,

$$bAb^{\mathrm{T}} = \sum_{i,j=0}^{P} b_i A_{ij} b_j = \sum_{i,j=0} b_i b_j \sum_{l=0} a_l e_{ijl} = \sum_{l=0} a_l \sum_{i,j=0} b_i b_j e_{ijl} = \sum_{l=0}^{P} a_l \sum_{i,j=0} b_i b_j E[\psi_i \psi_j \psi_l]$$

$$= E\left[\left(\sum_{l=0} a_l \psi_l\right)\left(\sum_{i=0} b_i \psi_i\right)\left(\sum_{j=0} b_j \psi_j\right)\right] = E[a_P(x,t,\xi)\beta(x,t,\xi)^2],$$

where $\beta(x,t,\xi) = \sum_{i=0}^{P} b_i \psi_i$. From the last expression, the theorem follows. $\square$

Note that the theorem implies that the boundary conditions for the derived system (4) are consistent with the boundary condition of the approximation of the original equation (3). To be specific, the theorem implies that all the new deterministic unknowns are outflow (or inflow) at one boundary if the projection of the original stochastic unknown is outflow (or inflow) under random fluctuations at the same boundary. Thus no non-physical conditions are introduced by the polynomial chaos expansion.

2.3. Computation of a smooth PDF

In this paper we adopt the method presented in [9], for recovering a 'smooth' PDF of any random variable based on a few samples. Assume that $f(x)$ is the PDF of a random variable at x, and $\{x_1,\ldots,x_N\}$ are N MC samples. Express $f(x)$ as a series of Legendre polynomials $\{P_n(x)\}$:

$$f(x) = \sum_{n=0}^{\infty} f_n P_n(x),$$

where

$$f_n = \frac{1}{\|P_n\|^2} \int_{-1}^{1} f(x) P_n(x).$$

Compute the above integration with the MC method, i.e.,

$$\int_{-1}^{1} f(x) P_n(x) \sim \frac{1}{N} \sum_{i=1}^{\infty} P_n(x_i).$$

Then a smooth probability density function is obtained as

$$f(x) \sim \frac{1}{N} \sum_{i=1}^{\infty} \sum_{n=0}^{\infty} \frac{1}{\|P_n\|^2} P_n(x_i) P_n(x) = \frac{K+1}{2N} \sum_{i=1}^{\infty} \frac{P_{K+1}(x) P_K(x_i) - P_K(x) P_{K+1}(x_i)}{x - x_i},$$

using the Christoffel-Darboux formula [15]. One should note that the adopted method is just a special orthogonal series estimator as reviewed in [8].

3. Steady-state inviscid burgers equation with source term

When an isentropic flow is choked in a dual-throat nozzle with equal throat areas, the steady flow can either be entirely supersonic, or subsonic, or contain a shock wave connecting the supersonic branch to the subsonic branch, depending on its initial state. In the latter case the shock location, is also determined by the initial state.

In [11] the following simplified model was analyzed:

$$\frac{\partial u}{\partial t} + \frac{\partial}{\partial x}\left(\frac{u^2}{2}\right) = \frac{\partial}{\partial x}\left(\frac{\sin^2 x}{2}\right), \quad 0 \leqslant x \leqslant \pi, \ t > 0, \tag{5}$$

with the initial condition

$$u(x,0) = \beta \sin x,$$

and boundary conditions

$$u(0,t) = u(\pi,t) = 0.$$

The exact steady-state solution to Eq. (5) is

$$u_{\infty}(x,\beta) = \lim_{t \to +\infty} u(x,\beta,t) = \begin{cases} u^+ = \sin x, & 0 < x \leqslant X_s, \\ u^- = -\sin x, & X_s < x < \pi. \end{cases} \tag{6}$$

The shock position X_s is a function of the parameter β in the initial condition

$$X_s = \begin{cases} \sin^{-1}\sqrt{1-\beta^2} & < \pi=2, \quad -1 < \beta \leqslant 0, \\ \pi - \sin^{-1}\sqrt{1-\beta^2} & > \pi=2, \quad 0 < \beta < 1. \end{cases} \tag{7}$$

When $|\beta| \geqslant 1$, $u_\infty(x,\beta)$ is smooth ($= \mathrm{sign}(\beta)\sin x$).

3.1. Initial condition I: one-dimensional Hermite chaos

Consider Eq. (5) with the initial condition

$$u(x,\beta,t=0) = \beta \sin x, \tag{8}$$

where β is a *random variable* defined as

$$\beta = \begin{cases} \frac{-1+\sqrt{1+4\alpha^2}}{2\alpha} & \text{if } \alpha \neq 0, \\ 0 & \text{if } \alpha = 0, \end{cases} \quad \text{or } \alpha = \frac{\beta}{1-\beta^2}. \tag{9}$$

Here α is a Gaussian random variable with the mean μ and standard variation σ, i.e., $\alpha \sim N(\mu,\sigma)$. The shock always exists in the steady state solution because $\beta \in (-1,1)$.

From (7), one finds that $\beta = -\cos(X_s)$, i.e.,

$$\alpha = \frac{-\cos(X_s)}{(\sin X_s)^2}. \tag{10}$$

The probability density function of the shock position X_s can therefore be computed directly as

$$\frac{1}{\sqrt{2\pi}\sigma} e^{-[(\alpha-\mu)^2=2\sigma^2]}\, d\alpha = p(X_s)dX_s \rightarrow p(X_s) = \frac{1}{\sqrt{2\pi}\sigma} e^{-[(\alpha-\mu)^2=2\sigma^2]} \frac{d\alpha}{d\beta}\frac{d\beta}{dX_s},$$

where $p(X_s)$ denotes the PDF of the shock position being at X_s. This yields

$$p(X_s) = \frac{1}{\sqrt{2\pi}\sigma} e^{-[(\alpha-\mu)^2=2\sigma^2]} \cdot \frac{1+\beta^2}{1-\beta^2{}^2}\sin(X_s), \quad 0 < X_s < \pi, \tag{11}$$

through $\beta = -\cos(X_s)$ and α as given by (10).

3.1.1. Hermite polynomial chaos solution

Since β is a function of a single Gaussian random variable, α, a one-dimensional Hermite polynomial chaos approximation ($n = 1$) suffices to represent the random function $u_\infty(x,\beta(\xi))$, i.e., we consider the expansion

$$u_\infty(x,\beta(\xi)) = \sum_{k=0}^{\infty} v_k(x)\psi_k(\xi). \tag{12}$$

Bear in mind that ξ is a Gaussian random variable with zero mean and unit variance. In the next theorem we will establish that this expansion converges. Surprisingly, although $u_\infty(x,\xi)$ is not smooth in the spatial variable x, all the coefficients $v_k(x)$ are smooth.

Theorem 2. (Smoothness). Let $u_\infty(x,\beta(\xi))$ be defined in (6). Let ξ be a Gaussian random variable with zero mean and unit variance and $\beta(\xi)$ is defined in (9). Then the expansion (12) converges and the coefficients $v_k(x)$ are smooth.

Proof. From the relations between α, ξ, β and the shock position X_s, one finds

$$\xi = \frac{1}{\sigma}\left(\frac{-\cos X_s}{(\sin X_s)^2} - \mu\right): \tag{13}$$

This implies that X_s is an increasing function of ξ and vice versa, when $0 < X_s < p$.

Let ξ_0 be the value of ξ which corresponds to the solution with shock position $x_0 \in (0, p)$, For a fixed x_0, the steady-state solution of (5) is given by

$$u_\infty(x_0, \xi) = \begin{cases} -\sin(x_0(\xi_0)) & \text{if } \xi \leq \xi_0, \\ \sin(x_0(\xi_0)) & \text{otherwise,} \end{cases} \tag{14}$$

because the shock position is an increasing function of ξ. Therefore,

$$\frac{1}{\sqrt{2p}}\int_{-\infty}^{+\infty}(u_\infty(x_0(\xi_0),\xi))^2 e^{-\xi^2/2}\,d\xi = (\sin x_0(\xi_0))^2 < +\infty,$$

and thus the expansion (12) converges in mean (see [4]).

The expansion coefficients are given by

$$v_k(x_0) = \frac{1}{\sqrt{2p}}\int_{-\infty}^{+\infty}u_\infty(x_0(\xi_0),\xi)\psi_k(\xi)e^{-\xi^2/2}\,d\xi = \frac{1}{\sqrt{2p}}\left(\int_{-\infty}^{\xi_0(x_0)} + \int_{\xi_0(x_0)}^{+\infty}\right)u_\infty(x_0(\xi_0),\xi)\psi_k(\xi)e^{-\xi^2/2}\,d\xi:$$

Plugging (14) into the above equation yields

$$v_k(x_0) = \frac{1}{\sqrt{2p}}\int_{-\infty}^{\xi_0}(-\sin x_0(\xi_0))\psi_k(\xi)e^{-\xi^2/2}\,d\xi + \int_{\xi_0}^{+\infty}\sin x_0(\xi_0)\psi_k(\xi)e^{-\xi^2/2}\,d\xi$$

$$= \frac{\sin x_0(\xi_0)}{\sqrt{2p}}\left(\int_{\xi_0(x_0)}^{+\infty} - \int_{-\infty}^{\xi_0(x_0)}\right)\psi_k(\xi)e^{-\xi^2/2}\,d\xi = \frac{\sin x_0(\xi_0)}{\sqrt{2p}}\left(d_k - 2\int_{-\infty}^{\xi_0(x_0)}\psi_k(\xi)e^{-\xi^2/2}\,d\xi\right), \tag{15}$$

where

$$d_k = \int_{+\infty}^{+\infty}\psi_k(\xi)e^{-\xi^2/2}\,d\xi = \delta_{k,0}$$

is independent of x_0. Denote the integral in (15) as $g(x_0)$. Using the chain rule, one can verify that

$$\frac{\partial g(x)}{\partial x} = \frac{\partial \xi}{\partial X_s}\Big|_{X_s=x} \cdot \psi_k(x)e^{-x^2/2},$$

from which one can see that $g(x)$ is a smooth function. The chain rule is valid because ξ is a smooth function of the shock position X_s on $(0, \pi)$ (see (13)). So we have proven that $v_k(x)$ is a smooth function of x for any k. $\square$

In Fig. 1, we show the first five Hermite polynomial chaos modes for the steady state solution of Eq. (5) when $\alpha \sim N(0, 0.1)$. Fig. 2 shows the absolute values of the first 21 Hermite polynomial chaos modes at the points 1.5708 and 1.3959. The slow decay is due to the discontinuity of the solution in the random space. The discontinuity in the random space can already be seen from Eq. (14). To emphasize this point, we draw a picture (Fig. 3) of the steady-state solution versus x and β, clearly showing the lack of smoothness in β.

To numerically solve Eq. (5) we seek a solution of the form

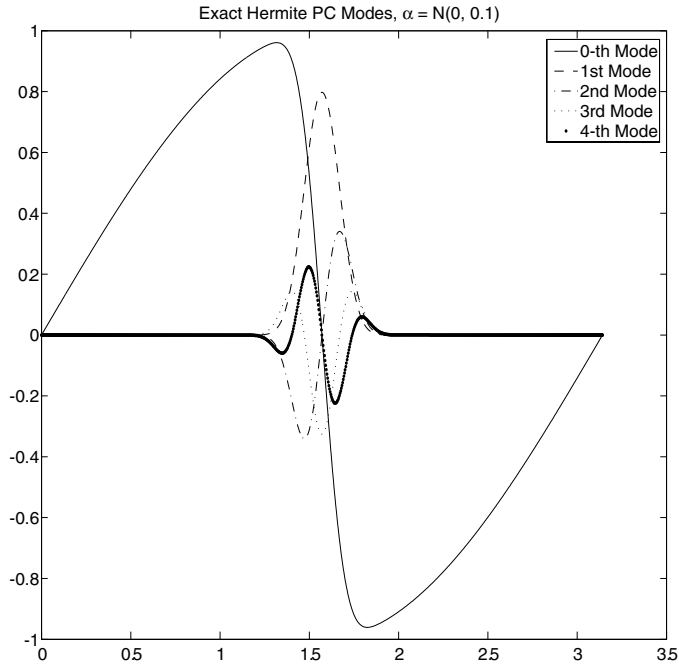$$u_p(x,\beta,t) = \sum_{k=0}^{X}v_k(x,t)\psi_k(\xi): \tag{16}$$

Fig. 1. The first five Hermite polynomial chaos modes for the steady-state solution of Eq. (5) when $\alpha \sim N(0,0.1)$.

Following the procedure outlined in Section 2.2.1 we obtain

$$\frac{\partial v_k}{\partial t} + \sum_{i,j=0}^{p} e_{ijk} \left(\frac{v_i v_j}{2} \right)_x = \delta_{k,0}(\sin x \cos x), \quad k = 0,1,\ldots,p, \tag{17}$$

where $\delta_{k,0}$ is the Kronecker delta function.

For this model problem, we want to compute the statistics of the shock position which is a derived quantity of the solution. The shock position does not have an analytical formula in general, although it has one (Eq. (7)) for the above special initial condition. For general cases, a bit more work has to be done in order to compute the statistics of the shock position. In polynomial chaos methods, it can be achieved by using a MC method on the computed solution (16). More precisely, we first generate a number of samples of ξ, and compute the realizations of the solution by the expansion. The shock position can then be extracted from each realization. Finally, we can compute the statistics of the shock positions.

Remark 1. The above procedure is very fast because only the series evaluation is involved in computing each realization.

3.1.1.1. Numerical results. Before solving Eq. (17), we check how accurately the Hermite polynomial chaos representation approximates the initial condition. The errors for $\alpha = N(0,0.1)$ and $N(0,0.3)$ are plotted in Fig. 4.

We have applied two schemes to solve Eq. (17): a first-order conservative finite difference (FD) scheme with a local Lax–Friedrich flux (LLF) [16] and a Chebyshev collocation method [6] with exponential filtering [17] in space. A third-order TVD Runge–Kutta scheme [13] has been used for the time discretization whenever Chebyshev collocation method is used for the spatial discretization. Otherwise, the first-order forward Euler scheme is used.

In the following figures, the 'exact PDF' is the probability density function from the analytical formula Eq. (11); the 'exact PDF from OSCM' is the PDF computed by the method given in Section 2.3 with a large number (20000 unless otherwise given) of samples. In this case, we first generate samples of β, compute the
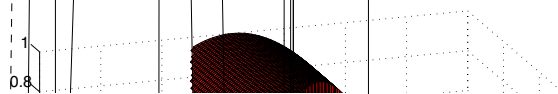
shock positions from the analytical formula, and then compute the probability density function by the method described in Section 2.3 from those shock positions. The '*p*th order PC' represents the probability density function computed with the same number of shock positions. This time, however, the shock positions are computed from the series expansion in the way as described above.

Fig. 5 presents the results obtained by the finite difference scheme. The accuracy of the probability density function is much worse than that obtained using the Chebyshev collocation method (Fig. 6). The main reason is the large dissipation of the scheme through the local Lax–Friedrich flux which depends
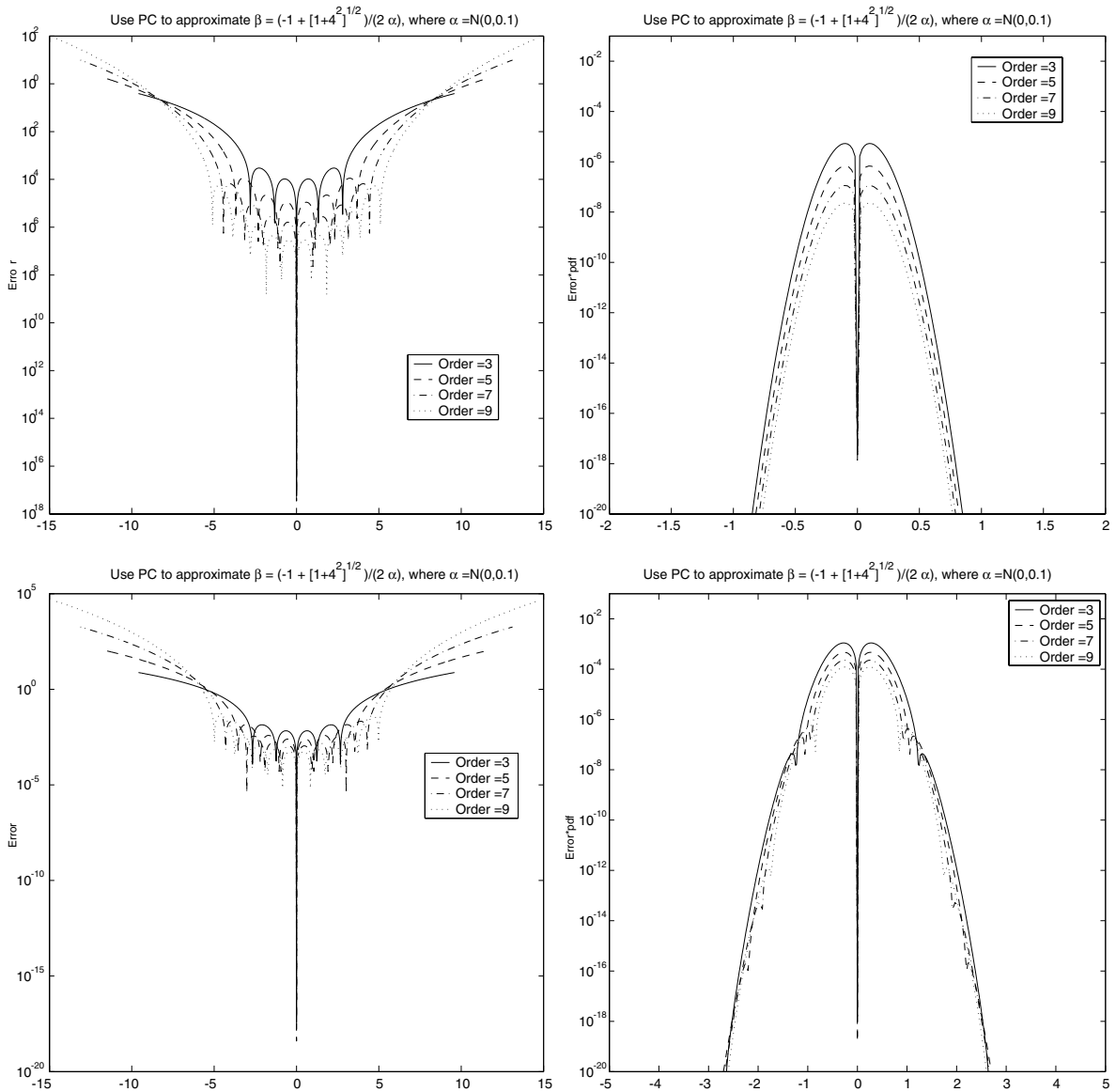
Fig. 4. Approximate $\beta = [(-1 + \sqrt{1 + 4\alpha^2})/2\alpha]$ with Hermite polynomials chaos expansion. (upper two pictures) $\alpha = N(0, 0.1)$; (lower two pictures) $\alpha = N(0, 0.3)$; (left two) the pointwise error; (right two) the product of the pointwise error and the PDF.
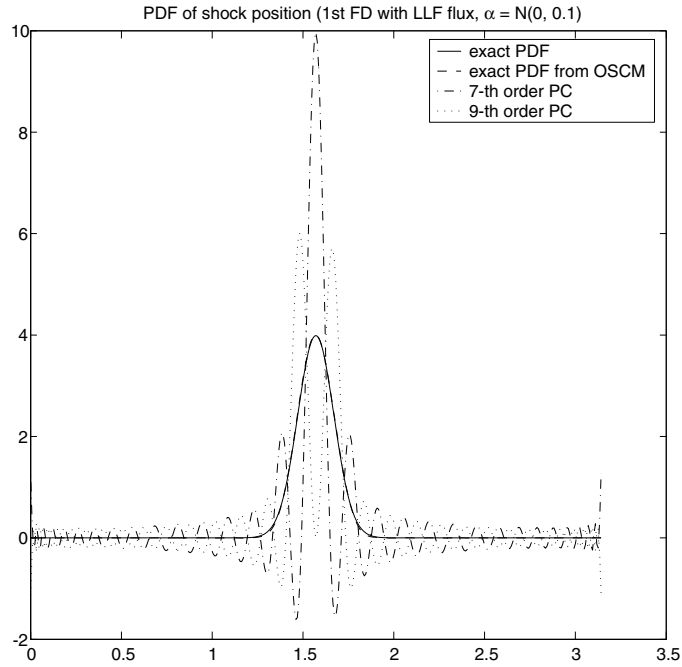
Fig. 5. PDF of shock positions from Hermite polynomial chaos methods. $\alpha = N(0,0.1)$. A first-order conservative scheme with local Lax–Friedrich flux is used for the spatial discretization. 1000 grid points on the domain $[0,p]$. CFL = 0.9.

on the eigenvalues of the flux-Jacobian of the system. Increasing the number of the Hermite polynomial chaos terms in the numerical solution of Eq. (17), increases the size of the system and the spectral radius (as shown in Table 1), and results in additional dissipation. (Note that the largest absolute eigenvalues in Table 1 are numerically computed.) Thus, the Chebyshev collocation method with $N = 128$ is used for the spatial discretization in the remaining numerical tests of the paper. And a sixth-order exponential filter is used in space unless specified otherwise.

The errors of up to the fourth-order moment of the shock position are also computed for the polynomial chaos method with a Chebyshev collocation method for the spatial discretization (see Fig. 7). When $\alpha \sim N(0,0.1)$, the errors are very small for the fifth- or higher order polynomial chaos methods. It is consistent with the PDF result in Fig. 6. For $\alpha \sim N(0,0.3)$ or $N(0,0.6)$, slow convergence is observed for high order moments. The spatial and time discretization errors dominate when the errors are small, thus the lack of improvement when increasing the polynomial chaos order p.

3.2. Initial condition II: one-dimensional Jacobi chaos

In this section we consider the initial condition (8) with β being a Beta random variable ($\beta \sim \text{Beta}(r,s)$) over the domain $[-1,1]$. For this initial random process, Jacobi polynomials are the natural choice for the polynomial chaos basis functions [19].

The probability density function of the shock locations X_s is

$$p(X_s) = \frac{(1+\beta)^{r-1}(1-\beta)^{s-1}}{2^{r+s-1}B(r,s)} \sin X_s, \quad 0 < X_s < p,$$

where $\beta = -\cos(X_s)$, $B(r,s) = \Gamma(r)\Gamma(s)\Gamma(r+s)$ is the Beta function, and $\Gamma(r)$ is the Gamma function.
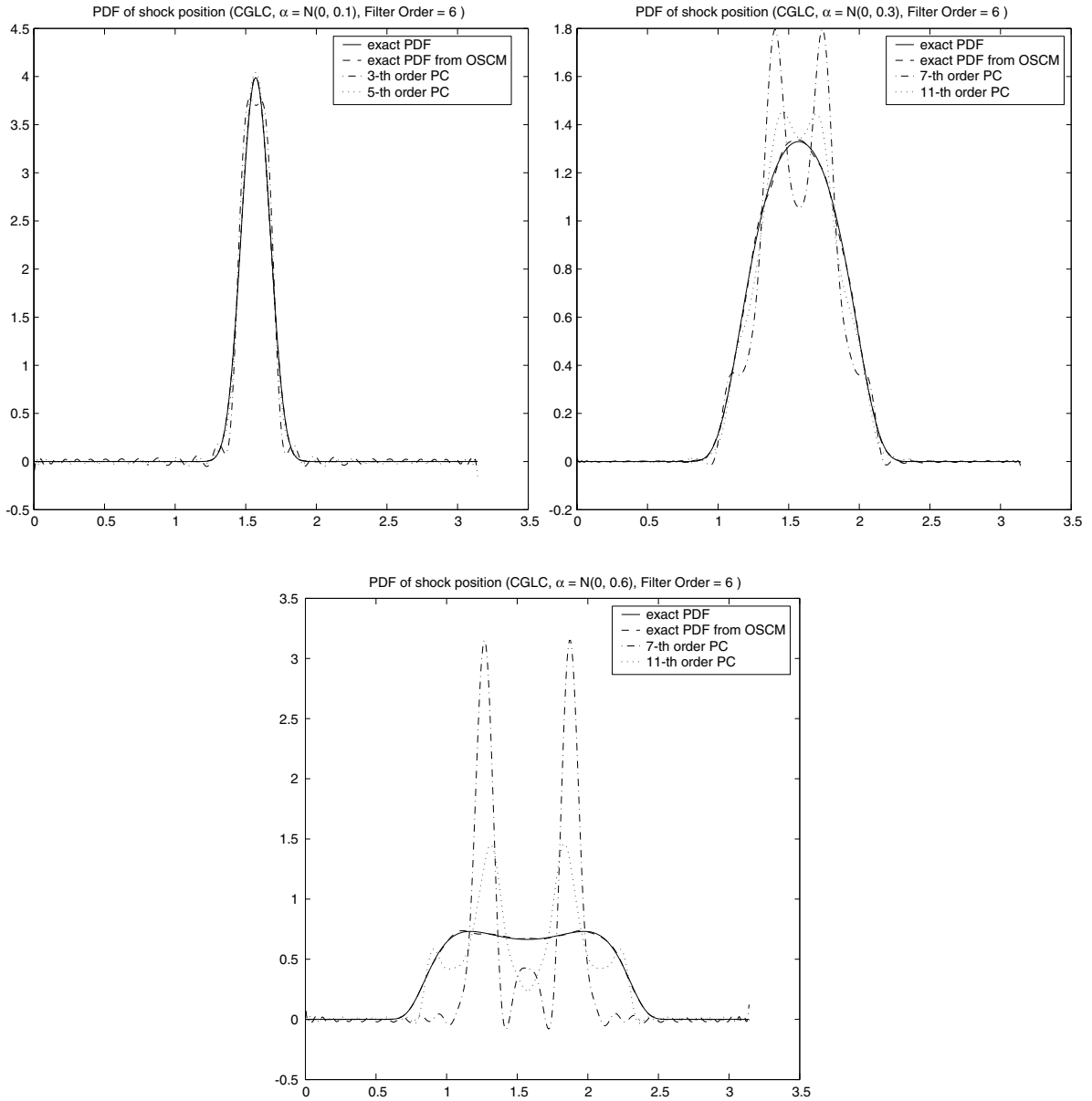
Fig. 6. PDF of shock positions from Hermite polynomial chaos methods. A Chebyshev collocation method with $N = 128$ is used for the spatial discretization. $Dt = (2=3p)N^{-2}$, where p is the order of the polynomial chaos. Exponential filter order is 6. (upper left) $\alpha = N(0, 0.1)$, 100,000 samples are used to compute the PDF; (upper right) $\alpha = N(0, 0.3)$, 100,000 samples are used to compute the PDF; (lower) $\alpha = N(0, 0.6)$, 200,000 samples are used to compute the PDF.

Similar to the Hermite polynomials chaos case, it is enough to use a one-dimensional Jacobi chaos expansion. The equations after applying the Galerkin procedure have the same form (17), but with the matrix e being computed from the Jacobi polynomials instead of the Hermite polynomials.

Table 1
Largest absolute eigenvalue (λ) of the flux-Jacobian matrix in Eq. (17) ($\alpha = N(0, 0.1)$)

PC Order	3	5	7	9	11
λ	3.41	6.95	19.04	29.07	42.24

1000 grid points is used in the spatial direction.
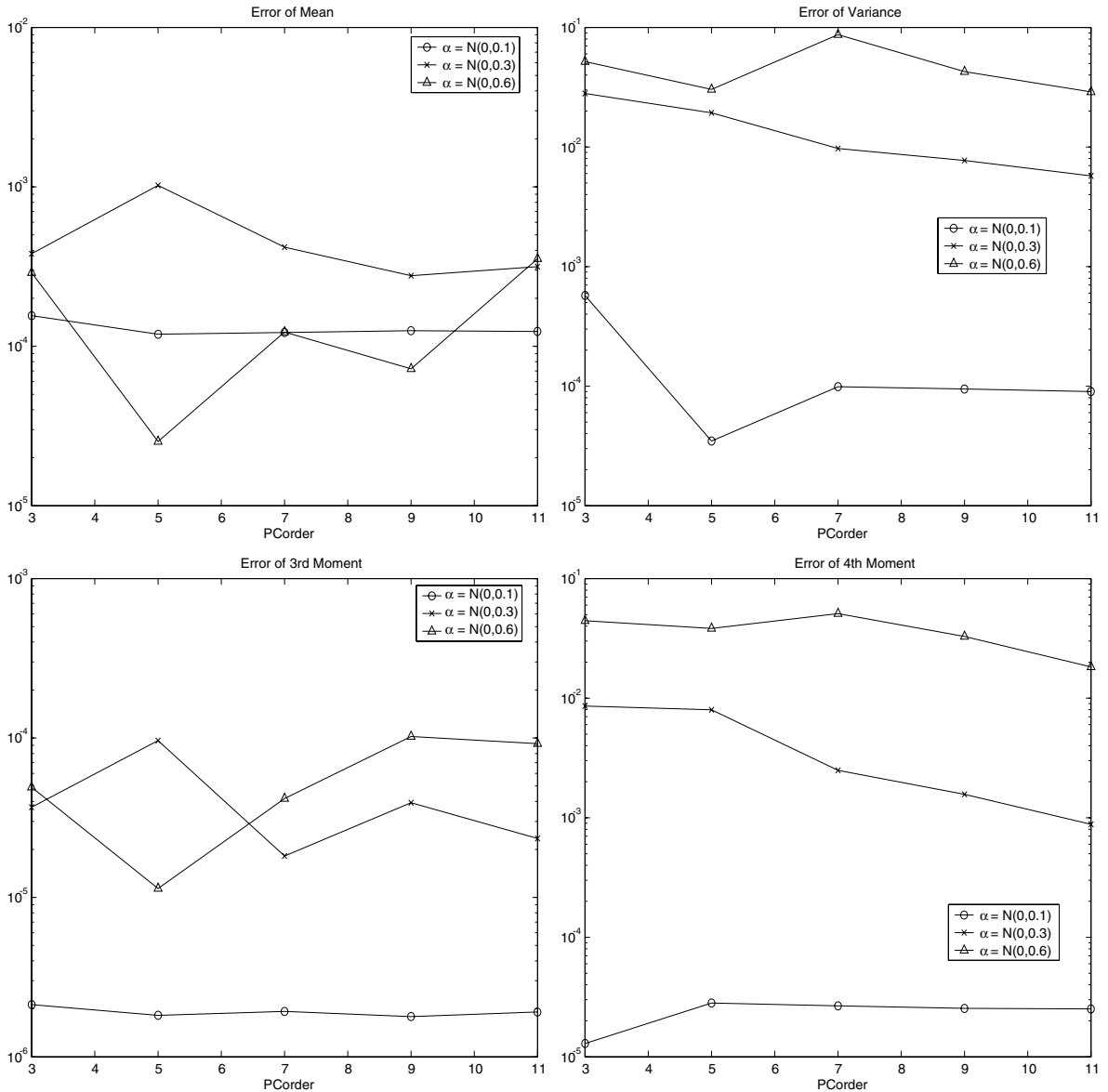
Fig. 7. Errors of up to the fourth moment of the shock position whose PDF is shown in Fig. 6. (upper left) Mean; (upper right) variance; (lower left) third moment (skewness); (lower right) fourth moment (kurtosis). (–O–) $\alpha \sim N(0, 0.1)$; (–×–) $\alpha \sim N(0, 0.3)$; (–△–) $\alpha \sim N(0, 0.6)$.

As before we can state

Theorem 3. (Smoothness). The coefficients in the Jacobi polynomial chaos expansion of the steady-state solutions are smooth.

Proof. The proof is omitted as it follows the approach in Theorem 2. □

In Figs. 8–11, we show the first five Jacobi polynomial chaos modes and the decay rate of the first 21 Jacobi polynomial chaos modes at some points for $r = s = 1$ and $r = s = 10$.

3.2.1. Numerical results

Since β is Beta distributed, there is no error introduced when expanding the initial condition into the Jacobi polynomial chaos basis functions. We test three different initial conditions: $\beta \sim \text{Beta}(1,1)$, $\text{Beta}(5,5)$, and $\text{Beta}(10,10)$. The results from the Chebyshev collocation method are shown in Fig. 12. When $\beta \sim \text{Beta}(10,10)$, the probability density function is computed with high accuracy. As the variance of β increases, many more Jacobi polynomial chaos terms (i.e., higher order polynomial chaos methods) are needed to produce reasonable results. This is because the solution is discontinuous in the random space and f is more localized for large r. (Note that β has PDF $\sim (1 - \beta^2)^r$ when $r = s$.)

3.3. Initial condition III: two-dimensional Hermite chaos

In this section we consider random *field* initial conditions of the form

$$u(x,\beta,t = 0) = \sigma(\sqrt{\lambda_1} f_1(x)\beta_1 + \sqrt{\lambda_2} f_2(x)\beta_2), \tag{18}$$

where β_1 and β_2 are functions of two independent identically distributed Gaussian random variables α_1 and α_2, respectively. The relations between α_i and β_i are given in (9). We assume that $\{\lambda_n\}$ and $\{f_n(x)\}$ take the form
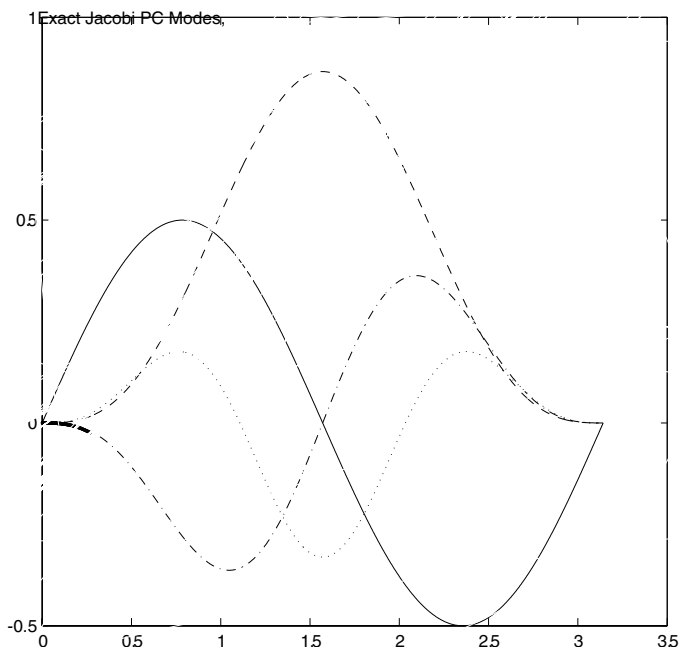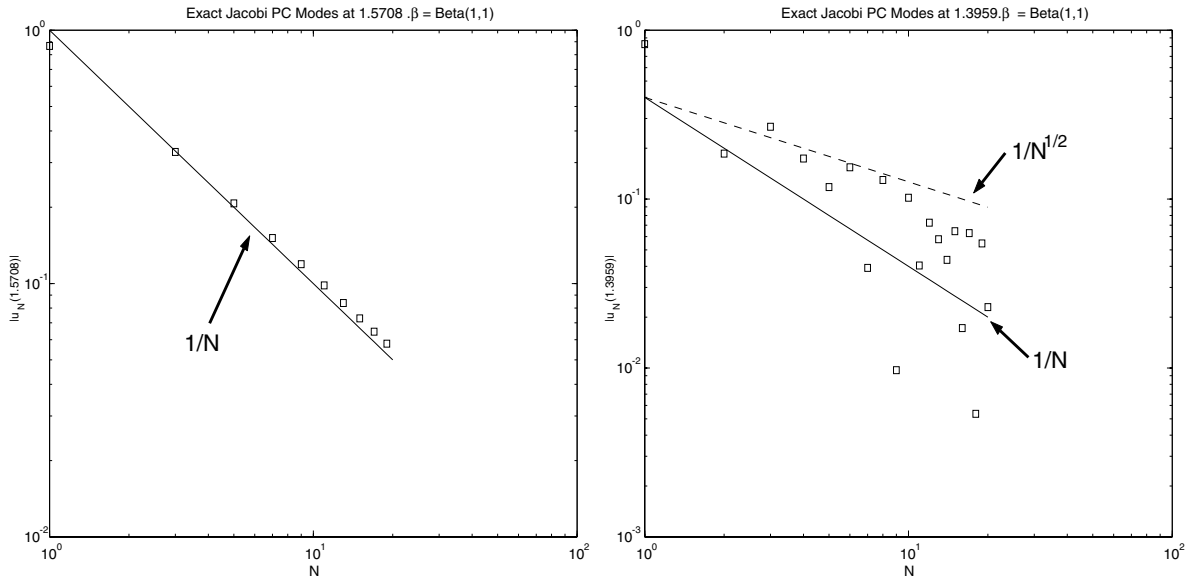
Fig. 9. Decay rate of the absolute values (at x) of the first 21 Jacobi polynomial chaos modes. $\beta \sim$ Beta$(1,1)$ on $[-1,1]$. (left) At the point $x = 1.5708$; (right) at the point $x = 1.3959$.
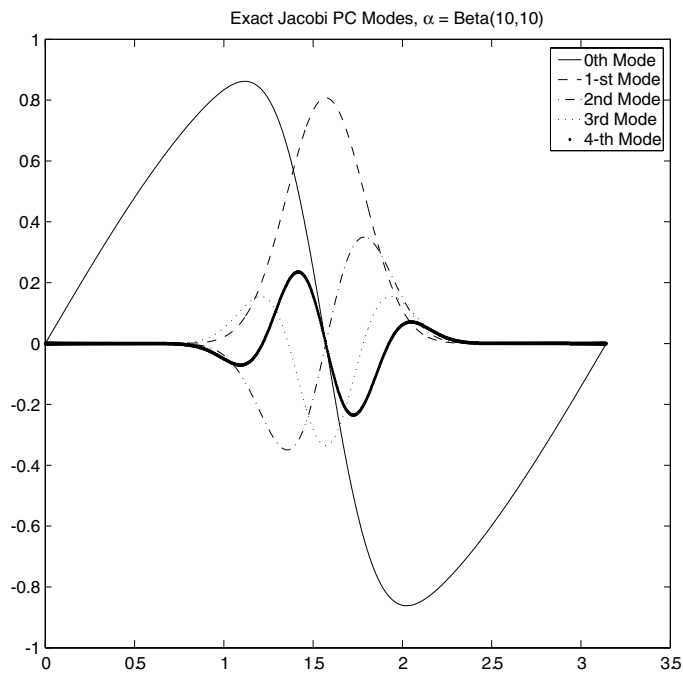

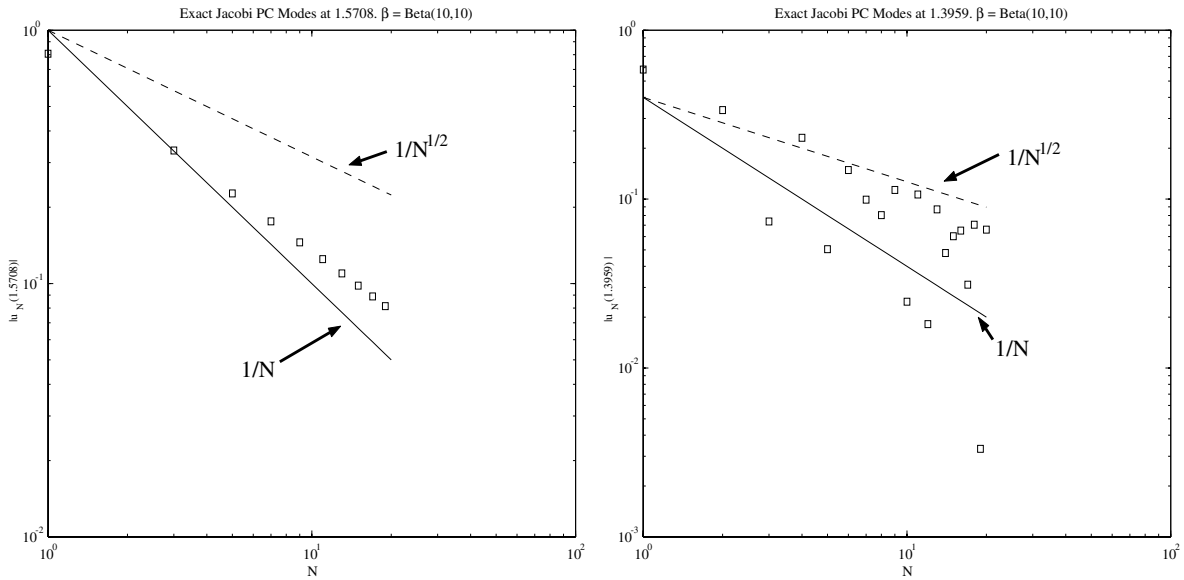Fig. 10. The first five Jacobi polynomial chaos modes, $r = s = 10$. $\beta \sim$ Beta(r,s) on $[-1,1]$.

Fig. 11. Decay rate of the absolute values (at x) of the first 21 Jacobi polynomial chaos modes, $r = s = 10$. $\beta \sim \text{Beta}(r,s)$ on $[-1,1]$. (left) At the point $x = 1.5708$; (right) at the point $x = 1.3959$.

$$\lambda_n = \frac{2b}{1 + b^2 \omega_n^2}, \quad n = 1,2,\ldots$$

and

$$f_n(x) = \begin{cases} \dfrac{\cos(\omega_n(x - p=2))}{a + \frac{\sin(2\omega_n a)}{2\omega_n}} & \text{if } n \text{ is odd,} \\ \dfrac{\sin(\omega_n(x - p=2))}{a - \frac{\sin(2\omega_n a)}{2\omega_n}} & \text{if } n \text{ is even,} \end{cases}$$

where $a = p/2$, $b = 10$, and the increasing sequence $\{\omega_n\}$ satisfies

$$\begin{cases} \frac{1}{b} - \omega_n \tan(\omega_n a) = 0 & \text{if } n \text{ is odd,} \\ \omega_n + \frac{1}{b} \tan(\omega_n a) = 0 & \text{if } n \text{ is even}: \end{cases}$$

Remark 2. The initial condition (18) (with $\sigma = 1$) given as above is the truncated Karhunen–Loève expansion of the exponential correlation [20] $C(x_1, x_2) = e^{-|x_1 - x_2|=b}$. One can refer to [5] for more details about the applicability of the Karhunen–Loève expansions in approximating the input random process.

Figs. 13 and 14 show the PDF of the shock positions for $\alpha_1, \alpha_2 \sim N(0, 0.1)$ and $N(0, 0.3)$ when $\sigma = 0.4$.

3.4. Initial condition IV: two-dimensional Jacobi chaos

As in Section 3.3, the initial condition takes the form (18). But instead, we assume β_1 and β_2 are Beta distributed. Numerical results for $\beta_1, \beta_2 \sim \text{Beta}(5, 5)$ and $\text{Beta}(10, 10)$ are shown in Figs. 15 and 16. One can see that the PDF from the polynomial chaos methods does appear to converge to the exact PDF, although it is still not very accurate for the eighth-order Jacobi chaos.
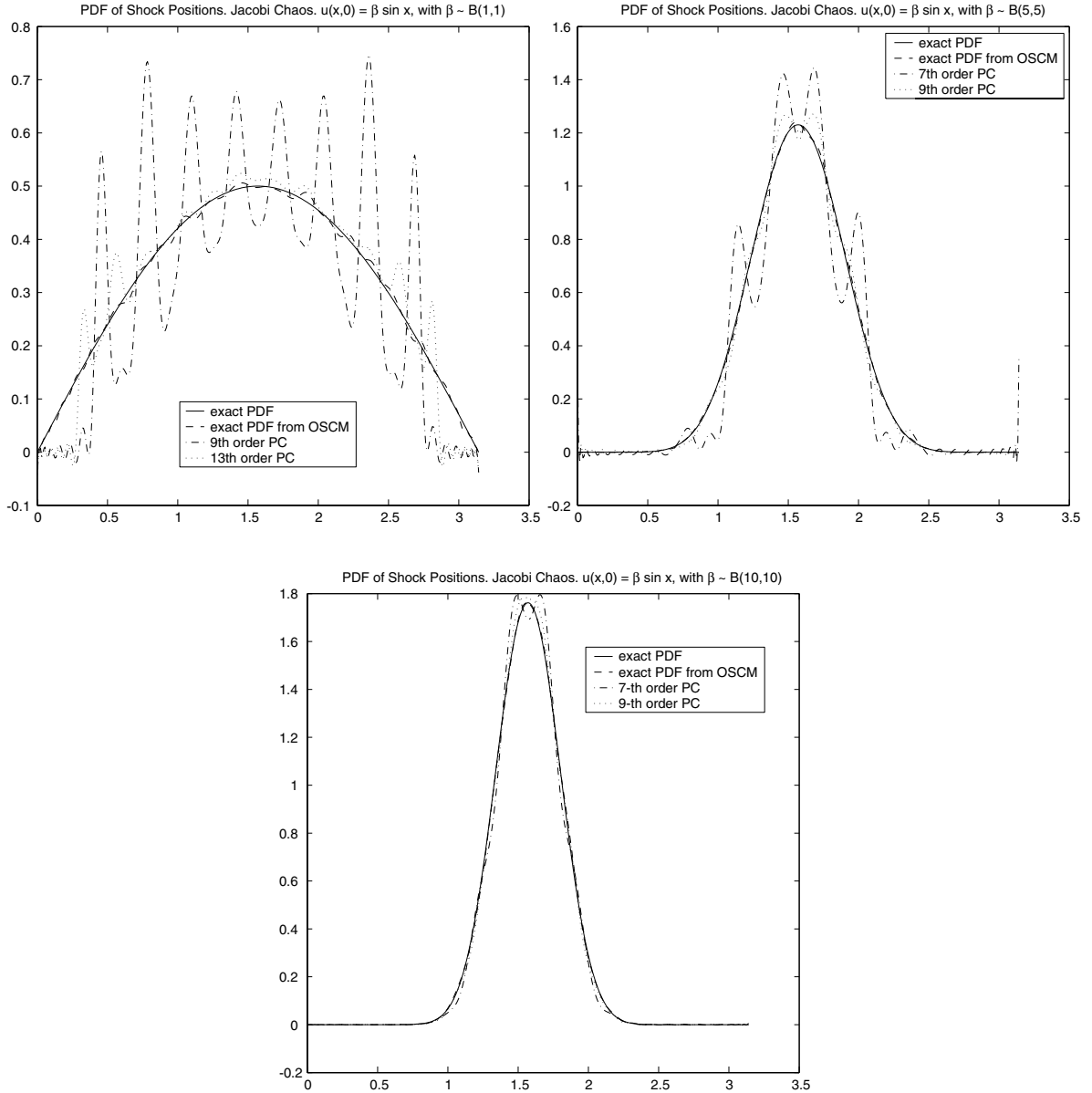
Fig. 12. PDF of shock positions from Jacobi polynomial chaos methods. 100,000 samples are used to compute the PDF. Other parameters are the same as used in Fig. 6. (upper left) β = Beta(1, 1); (upper right) β = Beta(5, 5); (lower) β = Beta(10, 10).

4. Summary

We have studied the effect of random initial conditions on the structure of the steady-state isentropic flow in a dual-throat nozzle with equal throat areas. Generalized polynomial chaos methods were implemented to analyze the uncertainty of the shock position for different stochastic initial conditions. Our main conclusions are:
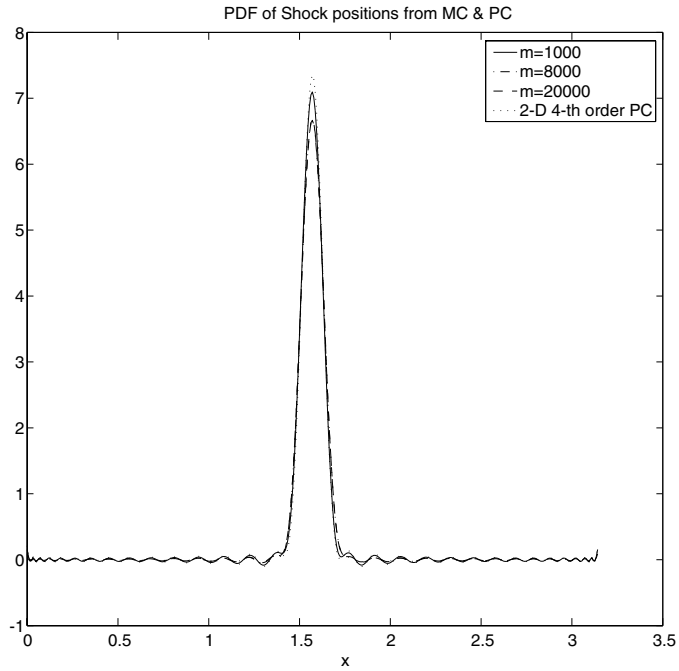
Fig. 13. PDF from MC with 1000, 8000, 20,000 samples and 2D fourth-order Hermite chaos method. D$t = N^{-1.5}$ for MC methods. D$t = (2/\{3[(n+p)!/n!p!]\})N^{-1.5}$ for the Hermite polynomial chaos methods. 20,000 samples are used to compute the PDF for the Hermite polynomial chaos methods with the method as described in Section 2.3. $\sigma = 0.4$. $\alpha_1, \alpha_2 \sim N(0, 0.1)$.
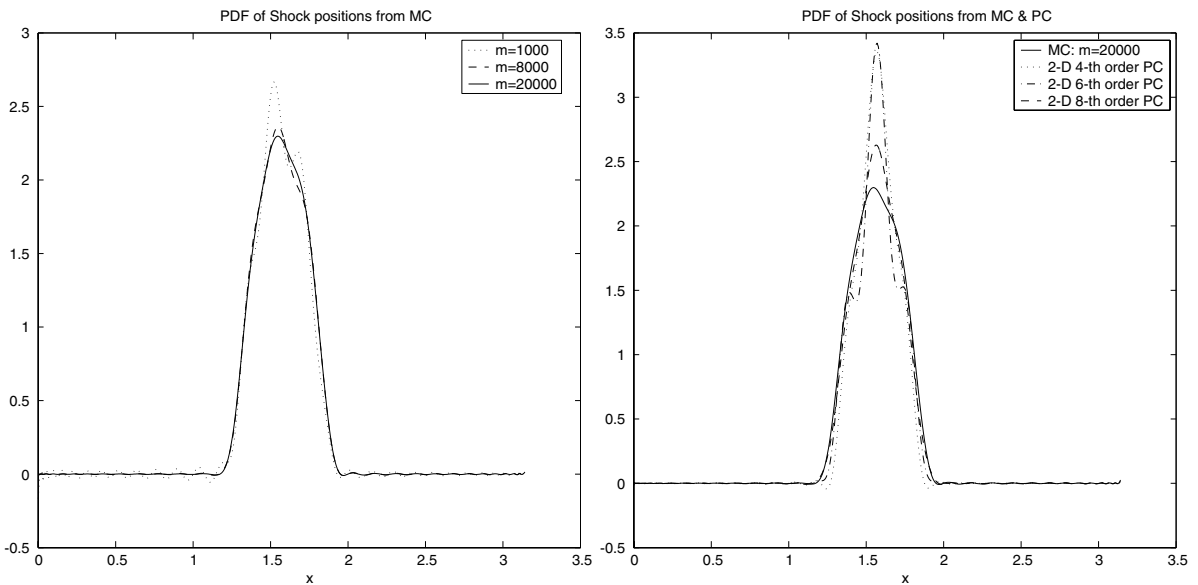

Fig. 14. PDF of shock positions. $\alpha_1, \alpha_2 \sim N(0, 0.3)$. All other parameters are the same as used in Fig. 13. (left) MC method with 1000, 8000, 20,000 samples; (right) fourth-, sixth-, eighth-order Hermite chaos.
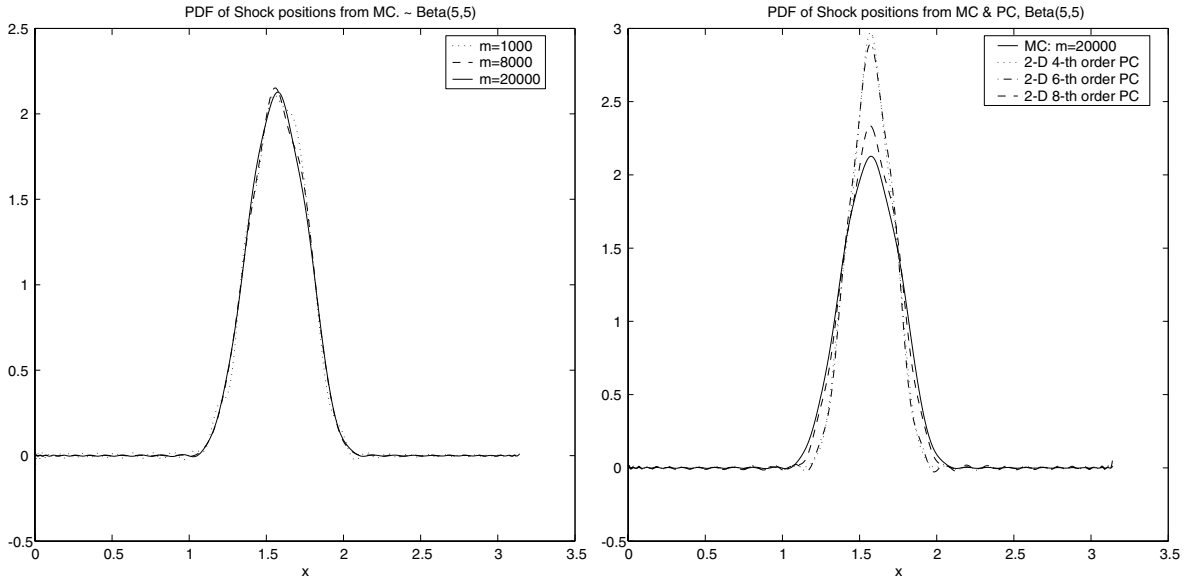
Fig. 15. PDF of shock positions. $\beta_1, \beta_2 \sim \text{Beta}(5, 5)$. All other parameters are the same used in Fig. 13. (left) MC method with 1000, 8000, 20,000 samples; (right) fourth-, sixth-, eighth-order Jacobi chaos.

- The polynomial chaos expansion modes are smooth functions of the spatial variable x, although the individual solution realizations are discontinuous in the spatial variable x.
- The solution is discontinuous in the random variable space at a fixed point x. Filtering is necessary for the stability of the scheme, as generalized polynomial chaos methods are spectral representations of the random processes.
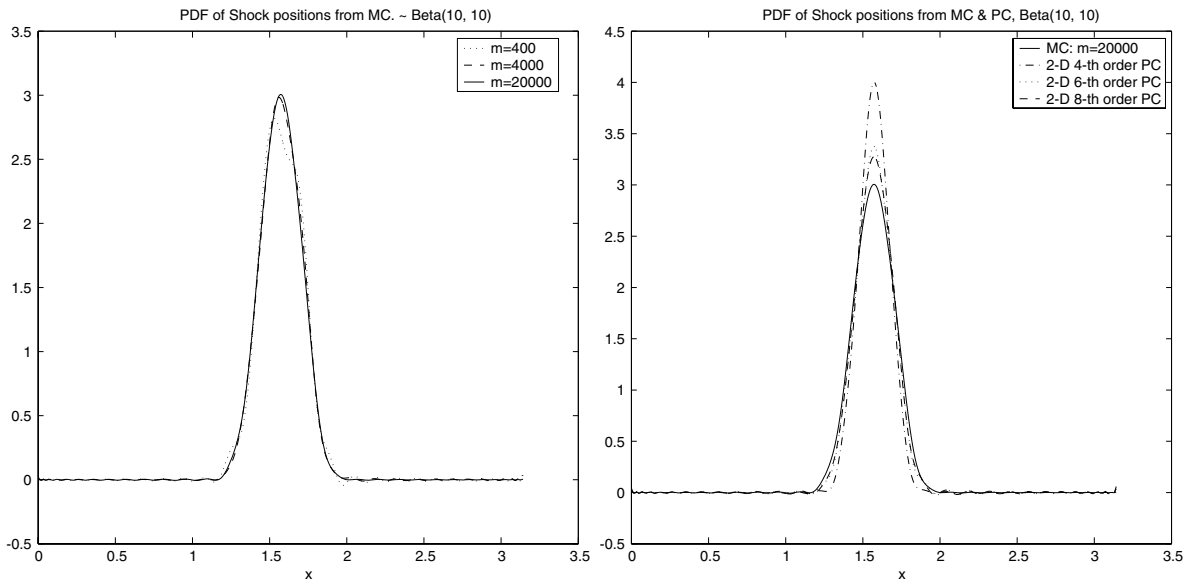

Fig. 16. PDF of shock positions. $\beta_1, \beta_2 \sim \text{Beta}(10, 10)$. All other parameters are the same as used in Fig. 13. (left) MC method with 400, 4000, 20,000 samples; (right) fourth-, sixth-, eighth-order Jacobi chaos.

- When the variance of the initial condition is small, the probability density function of the shock location is computed with high accuracy. Otherwise, many polynomial chaos expansion terms are needed to produce reasonable results. As first noted by Chorin [2], this is due to the slow convergence of the polynomial chaos expansions.
- The largest absolute eigenvalue of the flux-Jacobian matrix of the system increases quickly with respect to the number of the polynomial chaos terms used in the expansion. This might cause large dissipation for some numerical schemes. The increasing size of the system, when using more polynomial chaos terms, could also be problematic if one wants to solve the system with a high order numerical scheme using characteristic decomposition, e.g., high order ENO or WENO methods.

Acknowledgements

References

[1] R. Askey, J. Wilson, Some Basic Hypergeometric Polynomials that Generalize Jacobi PolynomialsMemoirs of the American Mathematical Society, 319, American Mathematical Society, Providence, RI, 1985.
[2] A.J. Chorin, Gaussian fields and random flow, Journal of Fluid Mechanics 63 (1974) 21–32.
[3] C.M. Dafermos, Trend to steady state in a conservation law with spatial inhomogeneity, Quarterly of Applied Mathematics XLV (2) (1987) 313–319.
[4] D. Funaro, Polynomial Approximation of Differential EquationsLecture Notes in Physics, Springer, New York, 1992.
[5] R.G. Ghanem, P.D. Spanos, Stochastic Finite Element: A Spectral Approach, Springer, New York, 1991.
[6] D. Gottlieb, S.A. Orszag, Numerical Analysis of Spectral Methods: Theory and ApplicationsCBMS-NSF Regional Conference Series in Applied Mathematics, SIAM, Philadelphia, PA, 1977.
[7] L. Huyse, R.W. Walters, Random field solutions including boundary condition uncertainty for the steady-state generalized burgers' equation, Report CR-2001-211239, ICASE, 2001.
[8] A.J. Izenman, Recent developments in nonparametric density estimation, Journal of the American Statistical Association 86 (413) (1991) 205–224.
[9] R.M. Jendrejack, J.J. de Pablo, M.D. Graham, A method for multiscale simulation of flowing complex fluids, Journal of Non-Newtonian Fluid Mechanics 108 (2002) 123–142.
[10] W.L. Oberkampf, J.C. Helton, K. Sentz, Mathematical representation of uncertainty, in: AIAA Non-Deterministic Approaches Forum, Seattle, WA, Paper No. 2001–1645, April 2001.
[11] M.D. Salas, S. Abarbanel, D. Gottlieb, Multiple steady states for characteristic initial value problems, Applied Numerical Mathematics 2 (1986) 193–210.
[12] G.I. Schuëller (Ed.), A State-of-the-art Report on Computational Stochastic Mechanics, Probabilistic Engineering Mechanics 12 (4) (1997) 197–321 (IASSAR Report).
[13] C.-W. Shu, A survey of strong stability preserving high order time discretizations, in: D. Estep, S. Tavener (Eds.), Collected Lectures on the Preservation of Stability under Discretization, SIAM, Philadelphia, PA, 2002, pp. 51–65.
[14] B. Sudret, A.D. Kiureghian, Stochastic finite element methods and reliability: a state-of-the-art report, Report UCB/SEMM-2000/08, Department of Civil & Environmental Engineering, University of California, Berkeley, November 2000.
[15] G. Szegö, Orthogonal Polynomials, fourth ed., American Mathematical Society, Providence, RI, 1975.
[16] E.F. Toro, Riemann Solvers and Numerical Methods for Fluid Dynamics: A Practical Introduction, fourth ed., Springer, New York, 1997.

[17] H. Vandeven, Family of spectral filters for discontinuous problems, Journal of Scientific Computing 6 (2) (1991) 159–192.
[18] R.W. Walters, L. Huyse, Uncertainty analysis for fluid mechanics with applications, Report CR-2002-211449, ICASE, 2002.
[19] D. Xiu, G.E. Karniadakis, Modeling uncertainty in flow simulations via generalized polynomial chaos, Journal of Computational Physics 187 (2003) 137–167.
[20] A.M. Yaglom, An Introduction to The Theory of Stationary Random Functions, Prentice-Hall, Englewood Cliffs, NJ, 1990.
[21] R. Ghanem, P. Spanos, Stochastic Finite Elements: A Spectral Approach, Springer Verlag, 1991.
[22] D. Xiu, G. Karniadakis, The Wiener-Askey Polynomial Chaos for Stochastic Differential Equations, SIAM J. Sci. Comp. 24 (2002) 619–644.